BIOCHEMISTRY

 Volume 44, Number 5 February 8, 2005

Accelerated Publications

No Evidence from FTIR Difference Spectroscopy That Aspartate-170 of the D1 Polypeptide Ligates a Manganese Ion That Undergoes Oxidation during the S_0 to S_1, S_1 to S_2, or S_2 to S_3 Transitions in Photosystem II†

Richard J. Debus,*,‡ Melodie A. Strickler,‡ Lee M. Walker,‡ and Warwick Hillier§

Department of Biochemistry, University of California, Riverside, California 92521-0129, and Research School of Biological Sciences, Australian National University, GPO Box 475, Canberra ACT, Australia 2601

Received November 19, 2004; Revised Manuscript Received December 23, 2004

ABSTRACT: On the basis of mutagenesis and X-ray crystallographic studies, Asp170 of the D1 polypeptide is widely believed to ligate the $(Mn)_4$ cluster that is located at the catalytic site of water oxidation in photosystem II. Recent proposals for the mechanism of water oxidation postulate that D1-Asp170 ligates a Mn ion that undergoes oxidation during one or more of the $S_0 \rightarrow S_1$, $S_1 \rightarrow S_2$, and $S_2 \rightarrow S_3$ transitions. To test these hypotheses, we have compared the FTIR difference spectra of the individual S state transitions in wild-type* PSII particles from the cyanobacterium *Synechocystis* sp. PCC 6803 with those in D1-D170H mutant PSII particles. Remarkably, our data show that the D1-D170H mutation does not significantly alter the mid-frequency regions (1800−1000 cm^{-1}) of *any* of the FTIR difference spectra. Therefore, we conclude that the oxidation of the $(Mn)_4$ cluster does not alter the frequencies of the carboxylate stretching modes of D1-Asp170 during the $S_0 \rightarrow S_1$, $S_1 \rightarrow S_2$, or $S_2 \rightarrow S_3$ transitions. The simplest explanation for these data is that the Mn ion that is ligated by D1-Asp170 does not increase its charge or oxidation state during any of these S state transitions. These data have profound implications for the mechanism of water oxidation. Either (1) the oxidation of the Mn ion that is ligated by D1-Asp170 occurs only during the transitory $S_3 \rightarrow S_4$ transition and serves as the critical step in the ultimate formation of the O−O bond or (2) the oxidation increments and O_2 formation chemistry that occur during the catalytic cycle involve only the remaining Mn_3Ca portion of the Mn_4Ca cluster. Our data also show that, if the increased positive charge on the $(Mn)_4$ cluster that is produced during the $S_1 \rightarrow S_2$ transition is delocalized over the $(Mn)_4$ cluster, it is not delocalized onto the Mn ion that is ligated by D1-Asp170.

The catalytic site of water oxidation in photosystem II (PSII)[1] contains a cluster of four Mn ions and one Ca ion. The $(Mn)_4$ cluster accumulates oxidizing equivalents in response to light-induced electron transfer reactions within PSII, thereby providing the interface between one-electron photochemistry and the four-electron process of water oxidation (for reviews, see refs *1*−*3*). The immediate oxidant of the $(Mn)_4$ cluster is tyrosine Y_Z. This residue transfers an electron from the $(Mn)_4$ cluster to $P_{680}^{\bullet+}$ in response to the light-induced formation of the latter. During each catalytic cycle, the $(Mn)_4$ cluster cycles through five oxidation states

† Support for this work was provided by the National Science Foundation (Grant MCB 0111065 to R.J.D.). Additional support to W.H. was provided by the Human Frontiers Science Program (Grant RGP0029/2002).

* To whom correspondence should be addressed. Phone: (951) 827-3483. Fax: (951) 827-4434. E-mail: richard.debus@ucr.edu.

‡ University of California.

§ Australian National University.

10.1021/bi047558u CCC: $30.25
Published on Web 01/14/2005

termed S_n, where "*n*" denotes the number of oxidizing equivalents that have been stored. The S_1 state predominates in dark-adapted samples. Most interpretations of Mn-XANES data have concluded that the S_1 state consists of two Mn(III) and two Mn(IV) ions and that the S_2 state consists of one Mn(III) and three Mn(IV) ions (for reviews, see refs *4* and *5*). Whether the additional oxidizing equivalent of the S_3 state is localized on a Mn ion (*6*−*8*) or on a Mn ligand (*4*, *5*, *9*, *10*) remains in dispute. The S_4 state is a transient intermediate that reverts to the S_0 state with the concomitant release of O_2.

In the most recent ∼3.5 Å (*11*) and ∼3.2 Å (*12*) X-ray crystallographic structural models of PSII, the electron density that corresponds to the $(Mn)_4Ca$ cluster is double lobed, with a single Mn ion being located in the smaller lobe and the remaining Mn ions and the Ca ion being located in the larger. Such an arrangement is compatible with simulations of EPR and ENDOR data that predicted the $(Mn)_4$ cluster to be arranged as three strongly exchange-coupled Mn ions that are weakly exchange-coupled to a fourth Mn ion (*13*). The precise arrangement of the individual Mn ions and their ligands differs in the ∼3.5 and ∼3.2 Å structural models. These differences are probably caused by differences in data quality, extent of radiation damage, and approach to interpreting the electron density. Regarding radiation damage, it has been determined that the high doses of X-rays that were employed for the crystallographic studies reduce the Mn ions and cause significant damage to the $(Mn)_4Ca$ complex.[2]

In terms of Mn ligation, the ∼3.5 and ∼3.2 Å structural models have four protein ligands in common. In both models, D1-Asp170 and D1-Glu333 ligate the Mn ion that is located in the smaller lobe of electron density. In the ∼3.5 Å model, both carboxylate residues are unidentate ligands (*11*). In the ∼3.2 Å model, both carboxylate residues are bidentate ligands, although D1-Asp170 is a strongly asymmetric bidentate ligand (*12*). In both models, D1-Glu189 and D1-His332 ligate one of the Mn ions that is located in the larger lobe of electron density. Of these four residues, D1-Asp170, D1-His332, and D1-Glu333 are among those that were identified as possible Mn ligands on the basis of earlier site-directed mutagenesis and chemical modification studies (for reviews, see refs *14*−*16*). In particular, ESEEM analyses of D1-H332E PSII particles from *Synechocystis* sp. PCC 6803 provided strong evidence in favor of Mn ligation by D1-His332 (*17*). Only the ligation of Mn by D1-Glu189 conflicts with the earlier mutagenesis studies (see the discussion in ref *16*).

It is known that D1-Asp170 provides part of the high-affinity binding site for the first Mn(II) ion that is photooxidized during the light-driven assembly of the $(Mn)_4$ cluster (*18*). On the basis of numerous mutagenesis studies, this residue is also thought to ligate the assembled $(Mn)_4$ cluster (*19*−*26*), although there is no conclusive spectroscopic evidence that this is so (*26*). Several studies have focused on the mutant D1-D170H. This mutant is weakly photoautotrophic and assembles $(Mn)_4$ clusters in ∼50% of its PSII reaction centers. The assembled $(Mn)_4$ clusters function normally (*19*, *22*, *23*), exhibit a normal mid-frequency (1800−1200 cm^{-1}) S_2-minus-S_1 FTIR difference spectrum (*25*), and exhibit normal S_1 and S_2 state multiline EPR signals (*26*).

Recent proposals for the mechanism of water oxidation in PSII postulate that D1-Asp170 ligates the Mn ion that undergoes oxidation during one or more of the $S_0 \rightarrow S_1$, $S_1 \rightarrow S_2$, and $S_2 \rightarrow S_3$ transitions (*27*−*30*). To test these hypotheses, we have compared the FTIR difference spectra of the $S_0 \rightarrow S_1$, $S_1 \rightarrow S_2$, $S_2 \rightarrow S_3$, and $S_3 \rightarrow S_0$ transitions in wild-type* PSII particles from the cyanobacterium *Synechocystis* sp. PCC 6803 with those in D1-D170H mutant PSII particles. FTIR difference spectroscopy is an extremely sensitive technique for characterizing dynamic structural changes that occur during an enzyme's catalytic cycle (*31*−*33*). These include changes in molecular interactions, protonation states, bonding (including changes in metal coordination and hydrogen bonding), bond strengths, and protein backbone conformations. In PSII, numerous vibrational modes change as the $(Mn)_4$ cluster is oxidized through the S state cycle (*34*−*39*). Identifying these modes will provide information about S state-dependent protein structural changes. This information is crucial to understanding the mechanism of water oxidation and will complement information that is being obtained from X-ray crystallography. On the basis of L-[1-^{13}C]alanine labeling of wild-type* and mutant PSII particles from *Synechocystis* sp. PCC 6803, we recently identified the symmetric carboxylate stretching mode of the α-COO^- group of D1-Ala344 in the S_2-minus-S_1 FTIR difference spectrum of wild-type* PSII particles (*40*). The frequency of this mode in the S_1 state and its ∼17 or ∼36 cm^{-1} downshift in the S_2 state imply that this group is a unidentate ligand of a Mn ion whose charge increases during the $S_1 \rightarrow S_2$ transition (*40*). A similar identification of one of the carboxylate stretching modes of D1-Asp170 in any of the $S_n \rightarrow S_{n+1}$ transitions could provide unequivocal spectroscopic evidence for the ligation of the $(Mn)_4$ cluster by D1-Asp170 and could provide information about the type of carboxylate ligation and the environment of the carboxylate group. If D1-Asp170 should ligate a Mn ion whose charge increases during a specific $S_n \rightarrow S_{n+1}$ transition, then the increased charge should weaken the ligating Mn−O bond(s), thereby decreasing the frequency of the D1-Asp170 symmetric carboxylate stretching mode and possibly shifting the frequency of the D1-Asp170 asymmetric carboxylate stretching mode. The shifted mode(s) should appear in the corresponding S_{n+1}-minus-S_n FTIR difference spectrum of wild-type* PSII particles but not in the spectrum of D1-

[1] Abbreviations: Chl, chlorophyll; EDTA, ethylenediaminetetraacetic acid; ENDOR, electron nuclear double resonance; EPR, electron paramagnetic resonance; ESEEM, electron spin−echo envelope modulation; EXAFS, extended X-ray absorption fine structure; FTIR, Fourier transform infrared; MES, 2-(*N*-morpholino)ethanesulfonic acid; NTA, nitrilotriacetic acid; P_{680}, chlorophyll species that serves as the light-induced electron donor in PSII; PSII, photosystem II; Q_A, primary plastoquinone electron acceptor; RH, relative humidity; TES, *N*-[tris(hydroxymethyl)methyl]-2-aminoethanesulfonic acid; wild-type*, control strain of *Synechocystis* sp. PCC 6803 that was constructed in identical fashion as the D1-D170H mutant but that contains the wild-type *psb*A-2 gene; XANES, X-ray absorption near edge structure; Y_Z, tyrosine residue that mediates electron transfer between the Mn cluster and $P_{680}^{\bullet+}$.

[2] The XANES of PSII single crystals shows that the Mn ions of the $(Mn)_4Ca$ complex are reduced to Mn(II) when the crystals are exposed to X-ray doses that are equivalent to those that were used for the X-ray crystallography experiments. In addition, the corresponding EXAFS data show that the intermetal Mn−Mn/Ca distances that are present in intact crystals are replaced by Mn−O interactions that are typical of Mn(II) complexes (V. K. Yachandra, personal communication).

D170H PSII particles, thereby permitting its (their) identification.

Our data show that the mid-frequency (1800−1000 cm^{-1}) S_1-minus-S_0, S_2-minus-S_1, S_3-minus-S_2, and S_0-minus-S_3 FTIR difference spectra of D1-D170H PSII particles are remarkably similar to those of wild-type* PSII particles. In particular, there is no indication that the D1-D170H mutation eliminates any carboxylate modes from any of these difference spectra. The simplest explanation for these data is that the Mn ion that is ligated by D1-Asp170 does not change its charge or oxidation state during the $S_0 \rightarrow S_1$, $S_1 \rightarrow S_2$, or $S_2 \rightarrow S_3$ transitions.

MATERIALS AND METHODS

Construction of the Site-Directed Mutant and Propagation of Cultures. The constructions of the D1-D170H mutant and wild-type* control strains were described previously (*25*). The designation "wild-type*" differentiates this strain from the native wild-type strain that contains all three *psb*A genes, lacks a His tag on the C-terminus of CP47, and is sensitive to antibiotics. Cells were propagated as described previously (*25*, *26*). To verify the integrity of the D1-D170H cultures that were harvested for the purification of PSII particles, an aliquot of each culture was set aside, and the complete sequence of the *psbA-2* gene was obtained after PCR amplification of genomic DNA (*22*). No traces of the wild-type D1-Asp170 codon nor of any spontaneous mutation within *psbA-2* (e.g., second site revertants) were detected.

Purification of PSII Particles. Isolated PSII particles were purified under dim green light at 4 °C with Ni-NTA superflow affinity resin (Qiagen, Valentia, CA) as described previously (*40*), except that the column was washed with only four volumes of purification buffer [25% (v/v) glycerol, 50 mM MES−NaOH (pH 6.0), 20 mM $CaCl_2$, 5 mM $MgCl_2$, 0.03% (w/v) *n*-dodecyl β-D-maltoside] before the purified PSII particles were eluted. Elution was accomplished in four column volumes with purification buffer containing 50 mM L-histidine. After the addition of EDTA to 1 mM, the eluted PSII particles were concentrated to 0.5−1.0 mg of Chl/mL by ultrafiltration (*26*), frozen in liquid nitrogen, and stored at −196 °C (vapor phase nitrogen).

Experimental Conditions for FTIR Measurements. All manipulations were conducted under dim green light at 4 °C. For each FTIR sample, approximately 30 μg of Chl was concentrated to <15 μL with a Microcon-100 concentrator (Millipore Corp., Bedford, MA). The concentrated sample was then diluted with 150 μL of FTIR buffer [40 mM sucrose, 10 mM MES−NaOH (pH 6.0), 5 mM $CaCl_2$, 5 mM NaCl, 0.06% (w/v) *n*-dodecyl β-D-maltoside (*39*)] and concentrated again. The sample was diluted and concentrated three to four additional times, with the final concentrated volume being approximately 10 μL. The concentrated sample was then mixed with $^1/_{10}$th volume of fresh 100 mM potassium ferricyanide (dissolved in water) and spread to a diameter of about 10 mm on a 15 mm diameter BaF_2 window. The sample was dried lightly (until tacky) under a stream of dry nitrogen gas. To maintain the humidity of the sample in the FTIR cryostat at 99% RH, 1 μL of 20% (v/v) glycerol (in water) was spotted onto the window, adjacent to the sample but not touching it (*36*−*39*). A second IR window with a Teflon spacer (0.5 mm thick) was placed over the first (the spacer was sealed to both windows with silicon-free high-vacuum grease). The sample was immediately loaded into the FTIR cryostat and allowed to equilibrate to 273.0 K in darkness for 2 h. The sample concentration and thickness were adjusted so that the absolute absorbance of the amide I band at 1657 cm^{-1} was 0.7−1.1.

FTIR Spectra. Mid-frequency FTIR spectra were recorded with a Bruker Equinox 55 spectrometer (Bruker Optics, Billerica, MA) that was equipped with a water-cooled globar source, a KBr beam splitter, a preamplified, midrange MCT detector (Model D316/6; InfraRed Associates, Stuart, FL), and a liquid nitrogen cryostat (Optistat DN; Oxford Instruments, Oxon, U.K.) that was controlled with an Oxford ITC502 temperature controller. This cryostat regulated the sample temperature to within ±0.1 K. One 2500 cm^{-1} long-pass Ge filter (Model FXLP-0400; Janos Technology, Townshend, VT) was mounted before the sample holder to reduce the spectral bandwidth and to prevent the interferometer's coaxial helium−neon laser beam from illuminating the sample. A second long-pass Ge filter was mounted after the sample holder to protect the MCT detector from scattered actinic illumination. Double-sided forward−backward interferograms were recorded with a scanner velocity of 80 kHz (this corresponds to a mirror velocity of 2.5 cm/s). For the calculation of Fourier transforms, a Blackmann-Harris three-term apodization function and a zero-fill factor of 4 were employed. The spectral resolution for all spectra was 4 cm^{-1}. Samples were illuminated with flashes (∼20 mJ/flash, ∼7 ns fwhm) from a frequency-doubled Q-switched Nd:YAG laser (Surelite I; Continuum, Santa Clara, CA). After dark adaptation, one preflash was applied followed by 5 min of additional dark adaptation (*39*). This treatment was employed to oxidize Y_D and to maximize the proportion of centers in the S_1 state. Then, six successive flashes were applied with an interval of 12.2 s between each. Two single-beam spectra (spaced by 12.2 s) were recorded before the first flash, and one single-beam spectrum was recorded starting 0.33 s after the first and subsequent flashes (each single-beam spectrum consisted of 100 scans). The 0.33 s delay was incorporated to allow for the oxidation of Q_A^- by the ferricyanide. To obtain difference spectra corresponding to successive S state transitions, the single-beam spectrum that was recorded after the *n*th flash was divided by the single-beam spectrum that was recorded immediately before the *n*th flash, and the ratio was converted to units of absorption. To estimate the background noise level, the second preflash single-beam spectrum was divided by the first, and the ratio was converted to units of absorption. The sample was dark adapted for 30 min, and then the entire cycle was repeated, including the preflash and the 5 min additional dark adaptation period. The entire cycle was repeated 10−12 times for each sample, and the difference spectra recorded with several samples were averaged.

RESULTS

The O_2 evolving activities of the purified wild-type* and D1-D170H PSII particles were 5.2−5.5 mmol of O_2 (mg of Chl)$^{-1}$ h^{-1} and 2.6−3.0 mmol of O_2 (mg of Chl)$^{-1}$ h^{-1}, respectively. The lower activity of the D1-D170H PSII particles (50−60% compared to wild type*) has been noted previously (*25*, *26*). The lower activity of the D1-D170H

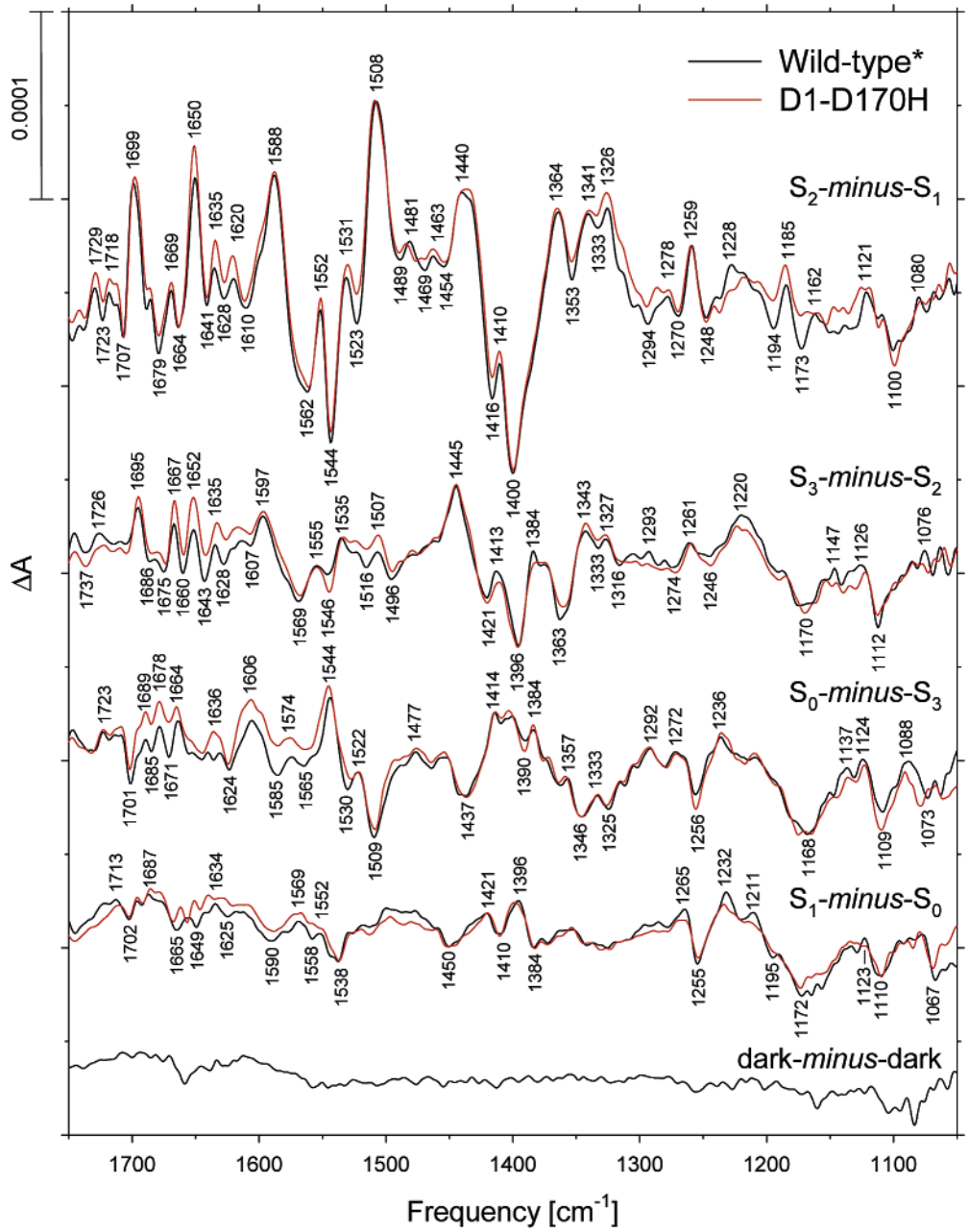

FIGURE 1: The mid-frequency FTIR difference spectra of wild-type* (black) and D1-D170H (red) PSII particles from *Synechocystis* sp. PCC 6803 in response to four successive flash illuminations. These spectra correspond predominantly to the S_2-minus-S_1, S_3-minus-S_2, S_0-minus-S_3, and S_1-minus-S_0 FTIR difference spectra, respectively. A dark-minus-dark control trace of the wild-type* PSII particles is included to show the noise level (lower trace). The data (plotted from 1750 to 1050 cm^{-1}) show the averages of 6 wild-type* and 18 D170H spectra. To facilitate comparisons, the D1-D170H spectra have been multiplied by factors of ~1.5 to maximize overlap with the wild-type* spectra. The samples included potassium ferricyanide as the electron acceptor. All spectra were collected with a sample temperature of 273 K and a resolution of 4 cm^{-1}.

PSII particles was expected because D1-D170H cells assemble $(Mn)_4$ clusters in only ~50% of their PSII reaction centers (*22*) and evolve O_2 at only ~50% the rate of wild-type* cells (*19*, *22*, *23*).

The mid-frequency FTIR difference spectra of wild-type* and D1-D170H PSII particles that were induced by four successive flash illuminations are shown in Figure 1 (black and red spectra, respectively). The spectra that were induced by the first, second, third, and fourth flashes correspond predominantly to the S_2-minus-S_1, S_3-minus-S_2, S_0-minus-S_3, and S_1-minus-S_0 FTIR difference spectra, respectively. The wild-type* spectra closely resemble the S_{n+1}-minus-S_n difference spectra that have been reported previously for *Synechocystis* sp. PCC 6803 (*39*) and are similar to those that have been reported for *Thermosynechococcus elongatus* (*34*, *36*−*38*) and spinach (*35*, *39*). The miss parameter also appears to be similar [this was estimated to be ~18% for *Synechocystis* sp. PCC 6803 (*39*) and 12−13% for *T. elongatus* (*34*, *36*)]. The control of sample humidity (*36*−*39*) and the inclusion of a preflash in the flash illumination protocol were essential for obtaining the spectra that are shown in Figure 1 and were employed in a previous study of PSII from this organism (*39*).

The amplitudes of the S_{n+1}-minus-S_n FTIR difference spectra of the D1-D170H PSII particles were only ~65% of the amplitudes of the corresponding difference spectra of

the wild-type* PSII particles. The lower amplitudes correlate approximately with the lower O_2 evolving activity of the D1-D170H PSII particles. To facilitate comparisons with the corresponding wild-type* spectra, the amplitudes of the D1-D170H spectra were normalized to those of the wild-type* spectra by multiplying the amplitudes of the D1-D170H spectra by factors of ~1.5.

A comparison of the normalized wild-type* and D1-D170H spectra (Figure 1) shows that the D1-D170H spectra are remarkably similar to the wild-type* spectra. The similarity of the S_2-minus-S_1 FTIR difference spectra of wild-type* and D1-D170H PSII particles between 1800 and 1200 cm^{-1} was noted previously (*25*). We have improved the S/N ratio of this earlier study. Furthermore, we now show that the S_2-minus-S_1, S_3-minus-S_2, S_0-minus-S_3, and S_1-minus-S_0 FTIR difference spectra of D1-D170H PSII particles are *all* remarkably similar to the corresponding FTIR difference spectra of wild-type* PSII particles. In particular, there are no significant differences between mutant and wild type* in the symmetric carboxylate stretching regions (1450−1300 cm^{-1}) of any of the spectra. Because this region is essentially free of overlapping bands from other functional groups (*40*), we conclude that the D1-D170H mutation eliminates none of the symmetric carboxylate stretching modes from *any* of the FTIR difference spectra. The minor differences that are observed between the wild-type* and D1-D170H spectra include small differences in the 1670−1630 cm^{-1} regions of the S_0-minus-S_3 and S_1-minus-S_0 difference spectra. These differences are contained within the amide I region (1690−1620 cm^{-1}) at frequencies that are high for asymmetric carboxylate modes (1640−1500 cm^{-1}). Further analyses will be required to determine if these differences correspond to altered amide I or asymmetric carboxylate modes. Importantly, these differences do not appear to represent the *elimination* of a vibrational mode in the D1-D170H mutant. Therefore, the D1-D170H mutation, in addition to eliminating none of the symmetric carboxylate stretching modes from any of the FTIR difference spectra, also appears to eliminate none of the asymmetric carboxylate stretching modes.

There is also no indication that the D1-D170H mutation produces new histidyl modes in any of the difference spectra [the C4═C5 and C5—N1 stretching modes of histidine appear at 1610−1565 cm^{-1} and near 1100 cm^{-1}, respectively (*41*, *42*)]. However, because histidyl bands are weak and overlap with amide I and carboxylate stretching modes [or with histidyl modes that are associated with the reduction of the non-heme Fe in a fraction of PSII reaction centers (*41*)], we cannot unambiguously exclude their presence without analyzing isotopically labeled samples. Nevertheless, because any histidyl modes that might be introduced by the D1-D170H mutation would replace the carboxylate modes of D1-Asp170, the fact that the mutation appears not to eliminate any carboxylate modes makes it unlikely that it introduces new histidyl modes.

DISCUSSION

Our FTIR data show that the D1-D170H mutation does not significantly alter the mid-frequency region (1800−1000 cm^{-1}) of *any* of the S_{n+1}-minus-S_n FTIR difference spectra in *Synechocystis* sp. PCC 6803. Therefore, *none* of the $S_0 \rightarrow S_1$, $S_1 \rightarrow S_2$, or $S_2 \rightarrow S_3$ transitions significantly alters the symmetric or asymmetric carboxylate stretching modes of D1-Asp170. This is an important and unexpected finding. The proximity of D1-Asp170 to Y_Z, to the Ca ion, and to charged amino acid residues that could serve in proton transfer pathways leading from the $(Mn)_4Ca$ cluster to the protein exterior has led to the idea that D1-Asp170 ligates the most catalytically active Mn ion in the $(Mn)_4Ca$ cluster (*11*, *28*−*30*).

We see three possible explanations for our FTIR data. First, D1-Asp170 does not ligate the *assembled* $(Mn)_4$ cluster. Second, D1-Asp170 ligates a Mn ion that undergoes oxidation during one or both of the $S_0 \rightarrow S_1$ and $S_2 \rightarrow S_3$ transitions,[3] but the increased charge on the Mn ion that undergoes oxidation is offset by the deprotonation of a water-derived ligand or water molecule that is bound to this Mn ion. Third, D1-Asp170 ligates a Mn ion that does not increase its charge or oxidation state during *any* of these $S_n \rightarrow S_{n+1}$ transitions.

The first possibility, that D1-Asp170 does not ligate the assembled $(Mn)_4$ cluster, seems unlikely, especially in view of the recent 3.5 Å (*11*) and 3.2 Å (*12*) structural models. Although it should be noted that no conclusive spectroscopic evidence exists showing that D1-Asp170 ligates the *assembled* $(Mn)_4$ cluster, it is known that D1-Asp170 forms part of the high-affinity binding site of the first Mn(II) ion that is photooxidized during the light-driven assembly of the $(Mn)_4$ cluster (*18*). Consequently, if D1-Asp170 does not ligate the *assembled* $(Mn)_4$ cluster, then a structural rearrangement must separate D1-Asp170 from the photooxidized Mn(III) ion as the $(Mn)_4$ cluster is formed. We know of no precedent for such a rearrangement in any metalloenzyme except ferritin, where the oxidation of two Fe(II) ions at the binuclear ferroxidase center is followed by transfer of a μ-oxo-bridged Fe(III) dimer to the ferrihydrite core (*43*, *44*). However, in ferritin, the change in Fe ligation environment is intimately associated with ferritin's function as an iron storage protein. In PSII, there is no apparent need for separating D1-Asp170 from Mn during the assembly of the $(Mn)_4$ cluster.

The second possibility, that Mn oxidation is compensated for by deprotonation events, has been proposed in some recent mechanistic models for water oxidation in PSII (*27*, *28*). In this scenario, D1-Asp170 ligates a Mn ion that undergoes oxidation during one or both of the $S_0 \rightarrow S_1$ and $S_2 \rightarrow S_3$ transitions, but the increased charge on the Mn ion that undergoes oxidation is offset by the deprotonation of a water-derived ligand or water molecule. We think that this scenario is incompatible with the totality of our FTIR data. First, all of the S_{n+1}-minus-S_n FTIR difference spectra exhibit a wealth of band shifts, showing that each S state transition subtly alters the vibrational modes of a variety of functional groups, including those of carboxylates and amides. Therefore, it seems highly improbable that replacing D1-Asp170 with the bulkier His residue would have no effect on these alterations. Second, the $S_2 \rightarrow S_3$ transition, whether

[3] We can exclude the possibility that D1-Asp170 ligates the Mn ion that undergoes oxidation during the $S_1 \rightarrow S_2$ transition because the uncompensated positive charge that develops on the $(Mn)_4$ cluster during the $S_1 \rightarrow S_2$ transition produces no significant shift of the carboxylate stretching modes of D1-Asp170. In contrast, this additional charge downshifts the symmetric carboxylate stretching mode of the α-COO^- group of D1-Ala344 by ~17 or ~36 cm^{-1} (*40*).

it is a Mn-centered oxidation (*6*−*8*) or a ligand-centered oxidation (*4*, *5*, *9*, *10*), is known to cause significant structural changes in the $(Mn)_4$ cluster: the ∼2.7 Å Mn−Mn distances increase to ∼2.8 and ∼3.0 Å and the ∼3.3 Å Mn−Mn/Ca distance increases by 0.04−0.2 Å (*45*). Some authors have proposed that an additional μ_2-oxo bridge is created during this transition (*8*, *30*). Another indication of the structural changes that occur during the $S_2 \rightarrow S_3$ transition is the markedly decreased susceptibility of the $(Mn)_4$ cluster to reduction by NH_2OH and NH_2NH_2 in the S_3 state (*46*, *47*). Small structural changes are also known to accompany the $S_0 \rightarrow S_1$ transition (*48*). If D1-Asp170 is a ligand of the Mn ion that undergoes oxidation during the $S_0 \rightarrow S_1$ or $S_2 \rightarrow S_3$ transitions, it seems highly unlikely that the structural changes that accompany these transitions would not also alter the vibrational modes of a carboxylate group (D1-Asp170) that is directly coordinated to the Mn ion that undergoes oxidation.

Therefore, we believe that the third possibility, that D1-Asp170 ligates a Mn ion that does not increase its charge or oxidation state during any of the $S_0 \rightarrow S_1$, $S_1 \rightarrow S_2$, or $S_2 \rightarrow S_3$ transitions, is the interpretation that is most consistent with our FTIR data. This conclusion has profound implications for the mechanism of water oxidation in PSII. Either the oxidation of the Mn ion that is ligated by D1-Asp170 occurs only during the transitory $S_3 \rightarrow S_4$ transition and serves as the critical step in the ultimate formation of the O−O bond or the oxidation increments and O_2 formation chemistry that occur during the catalytic cycle involve only the remaining Mn_3Ca portion of the Mn_4Ca cluster. These conclusions contradict the recent mechanistic proposals (*28*−*30*) that derive from the recent X-ray crystallographic structural models (*11*, *12*).

In a previous FTIR study, we identified the symmetric carboxylate stretching mode of the α-COO^- group of D1-Ala344 in the S_2-minus-S_1 FTIR difference spectrum (*40*). The frequency of this mode in the S_1 state and its ∼17 or ∼36 cm^{-1} downshift in the S_2 state imply that this group is a unidentate ligand of a Mn ion whose charge increases during the $S_1 \rightarrow S_2$ transition. Assuming that the extra oxidizing equivalent of the S_2 state is localized primarily on a single Mn(IV) ion that is produced during the $S_1 \rightarrow S_2$ transition, we suggested that the α-COO^- group of D1-Ala344 ligates the Mn ion that is oxidized during the $S_1 \rightarrow S_2$ transition (*40*). However, on the basis of recent resonant inelastic X-ray scattering (RIXS) measurements (*49*), it has been argued that the electron that is removed from the $(Mn)_4$ cluster during the $S_1 \rightarrow S_2$ transition originates from a strongly delocalized orbital. If so, then the extra positive charge that is created during this transition is spread over multiple Mn ions. Because our data show that neither carboxylate stretching mode of D1-Asp170 is shifted significantly during the $S_1 \rightarrow S_2$ transition, we conclude that any delocalization of this extra charge does not extend onto the Mn ion that is ligated by D1-Asp170.

In an earlier study, we showed that the D1-D170H mutation shifts a low-frequency S_2 state mode from ∼606 to ∼612 cm^{-1} (*25*). Because this mode is also shifted by the substitution of Sr^{2+} for Ca^{2+} (and by the exchange of $H_2{}^{18}O$ for $H_2{}^{16}O$) but not by the substitution of $^{44}Ca^{2+}$ for $^{40}Ca^{2+}$ (*50*), we concluded that the D1-D170H mutation introduces a subtle structural perturbation into the $(Mn)_4$ core (*25*). The remarkable similarity of the mid-frequency S_{n+1}-minus-S_n FTIR difference spectra of wild-type* and D1-D170H PSII particles shows that the Mn carboxylate ligands whose vibrational modes change during the $S_0 \rightarrow S_1$, $S_1 \rightarrow S_2$, or $S_2 \rightarrow S_3$ transitions are largely insensitive to this structural perturbation. Analyses of $(Mn)_4$ model compounds that resemble the $(Mn)_4$ cluster in PSII will be required to provide further insight into the nature of the ∼606 cm^{-1} mode and into the coupling of protein ligand modes with the $(Mn)_4$ core.

CONCLUDING REMARKS

The S_{n+1}-minus-S_n FTIR difference spectra of D1-D170H PSII particles are remarkably similar to those of wild-type* PSII particles. In particular, there is no indication that the D1-D170H mutation eliminates any carboxylate modes. The simplest explanation of these data is that D1-Asp170 ligates a Mn ion that does not increase its charge or oxidation state during any of the $S_0 \rightarrow S_1$, $S_1 \rightarrow S_2$, or $S_2 \rightarrow S_3$ transitions. The similarity of the wild-type* and mutant S_2-minus-S_1 FTIR difference spectra implies that any delocalization of the positive charge that is created during the $S_1 \rightarrow S_2$ transition does not extend to the Mn ion that is ligated by D1-Asp170.

ACKNOWLEDGMENT

We are grateful to Anh P. Nguyen for expert technical assistance, to Taka-aki Ono for helpful advice and for sharing ref *39* prior to its publication, and to David F. Bocian for valuable discussions.

REFERENCES

1. Goussias, C., Boussac, A., and Rutherford, A. W. (2002) Photosystem II and Photosynthetic Oxidation of Water: An Overview, *Philos. Trans. R. Soc. London, Ser. B 357*, 1369−1381.
2. Sauer, K., and Yachandra, V. K. (2004) The Water-Oxidation Complex in Photosynthesis, *Biochim. Biophys. Acta 1655*, 140−148.
3. Vrettos, J. S., and Brudvig, G. W. (2004) Oxygen Evolution, *Compr. Coord. Chem. II 8*, 507−547.
4. Yachandra, V. K. (2002) Structure of the Manganese Complex in Photosystem II: Insights from X-ray Spectroscopy, *Philos. Trans. R. Soc. London, Ser. B 357*, 1347−1358.
5. Yachandra, V. K. (2005) The Catalytic Manganese Cluster, in *Photosystem II: The Water/Plastoquinone Oxido-Reductase of Photosynthesis* (Wydrzynski, T., and Satoh, K., Eds.) Kluwer Academic Publishers, Dordrecht, The Netherlands (in press).
6. Ono, T.-A., Noguchi, T., Inoue, Y., Kusunoki, M., Matsushita, T., and Oyanagi, H. (1992) X-ray Detection of the Period-Four Cycling of the Manganese Cluster in Photosynthetic Water Oxidizing Enzyme, *Science 258*, 1335−1337.
7. Iuzzolino, L., Dittmer, J., Dörner, W., Meyer-Klaucke, W., and Dau, H. (1998) X-ray Absorption Spectroscopy on Layered Photosystem II Membrane Particles Suggests Manganese-Centered Oxidation of the Oxygen-Evolving Complex for the S_0-S_1, S_1-S_2, and S_2-S_3 Transitions of the Water Oxidation Cycle, *Biochemistry 37*, 17112−17119.
8. Dau, H., Iuzzolino, L., and Dittmer, J. (2001) The Tetra-Manganese Complex of Photosystem II during its Redox Cycle−X-ray Absorption Results and Mechanistic Implications, *Biochim. Biophys. Acta 1503*, 24−39.
9. Roelofs, T. A., Liang, W., Latimer, M. J., Cinco, R. M., Rompel, A., Andrews, J. C., Sauer, K., Yachandra, V. K., and Klein, M. P. (1996) Oxidation States of the Manganese Cluster During the Flash-Induced S-state Cycle of the Photosynthetic Oxygen-Evolving Complex, *Proc. Natl. Acad. Sci. U.S.A. 93*, 3335−3340.
10. Messinger, J., Robblee, J. H., Bergmann, U., Fernandez, C., Glatzel, P., Visser, H., Cinco, R. M., McFarlane, K. L., Bellacchio, E., Pizarro, S. A., Cramer, S. P., Sauer, K., Klein, M. P., and

Yachandra, V. K. (2001) Absence of Mn-Centered Oxidation in the $S_2 \rightarrow S_3$ Transition: Implications for the Mechanism of Photosynthetic Water Oxidation, *J. Am. Chem. Soc. 123*, 7804−7820.

11. Ferreira, K. N., Iverson, T. M., Maghlaoui, K., Barber, J., and Iwata, S. (2004) Architecture of the Photosynthetic Oxygen-Evolving Center, *Science 303*, 1831−1838.
12. Biesiadka, J., Loll, B., Kern, J., Irrgang, K.-D., and Zouni, A. (2004) Crystal Structure of Cyanobacterial Photosystem II at 3.2 Å Resolution: A Closer Look at the Mn-Cluster, *Phys. Chem. Chem. Phys. 6*, 4733−4736.
13. Peloquin, J. M., Campbell, K. A., Randall, D. W., Evanchik, M. A., Pecoraro, V. L., Armstrong, W. H., and Britt, R. D. (2000) ^{55}Mn ENDOR of the S_2-state Multiline EPR Signal of Photosystem II: Implications on the Structure of the Tetranuclear Mn Cluster, *J. Am. Chem. Soc. 122*, 10926−10942.
14. Diner, B. A. (2001) Amino Acid Residues Involved in the Coordination and Assembly of the Manganese Cluster of Photosystem II. Proton-Coupled Electron Transport of the Redox-Active Tyrosines and Its Relationship to Water Oxidation, *Biochim. Biophys. Acta 1503*, 147−163.
15. Debus, R. J. (2001) Amino Acid Residues that Modulate the Properties of Tyrosine Y_Z and the Manganese Cluster in the Water Oxidizing Complex of Photosystem II, *Biochim. Biophys. Acta 1503*, 164−186.
16. Debus, R. J. (2005) The Catalytic Manganese Cluster—II. Protein Ligation, in *The Water/Plastoquinone Oxido-Reductase of Photosynthesis* (Wydrzynski, T., and Satoh, K., Eds.) Kluwer Academic Publishers, Dordrecht, The Netherlands (in press).
17. Debus, R. J., Campbell, K. A., Gregor, W., Li, Z.-L., Burnap, R. L., and Britt, R. D. (2001) Does Histidine 332 of the D1 Polypeptide Ligate the Manganese Cluster in Photosystem II? An Electron Spin−Echo Envelope Modulation Study, *Biochemistry 40*, 3690−3699.
18. Campbell, K. A., Force, D. A., Nixon, P. J., Dole, F., Diner, B. A., and Britt, R. D. (2000) Dual-Mode EPR Detects the Initial Intermediate in Photoassembly of the Photosystem II Mn Cluster: The Influence of Amino Acid Residue 170 of the D1 Polypeptide on Mn Coordination, *J. Am. Chem. Soc. 122*, 3754−3761.
19. Nixon, P. J., and Diner, B. A. (1992) Aspartate 170 of the Photosystem II Reaction Center Polypeptide D1 is Involved in the Assembly of the Oxygen-Evolving Manganese Cluster, *Biochemistry 31*, 942−948.
20. Diner, B. A., and Nixon, P. J. (1992) The Rate of Reduction of Oxidized Redox-Active Tyrosine, Z+, by Exogenous Mn^{2+} is Slowed in a Site-Directed Mutant, at Aspartate 170 of Polypeptide D1 of Photosystem II, Inactive for Photosynthetic Oxygen Evolution, *Biochim. Biophys. Acta 1101*, 134−138.
21. Boerner, R. J., Nguyen, A. P., Barry, B. A., and Debus, R. J. (1992) Evidence from Directed Mutagenesis that Aspartate 170 of the D1 Polypeptide Influences the Assembly of the Manganese Cluster in the Photosynthetic Water-Splitting Complex, *Biochemistry 31*, 6660−6672.
22. Chu, H.-A., Nguyen, A. P., and Debus, R. J. (1994) Site-Directed Photosystem II Mutants with Perturbed Oxygen Evolving Properties: 1. Instability or Inefficient Assembly of the Manganese Cluster *In Vivo*, *Biochemistry 33*, 6137−6149.
23. Whitelegge, J. P., Koo, D., Diner, B. A., Domian, I., and Erickson, J. M. (1995) Assembly of the Photosystem II Oxygen-Evolving Complex is Inhibited in *psb*A Site-Directed Mutants of *Chlamydomonas reinhardtii*, *J. Biol. Chem. 270*, 225−235.
24. Chu, H.-A., Nguyen, A. P., and Debus, R. J. (1995) Amino Acid Residues that Influence the Binding of Manganese or Calcium to Photosystem II. 1. The Lumenal Inter-Helical Domains of the D1 Polypeptide, *Biochemistry 34*, 5839−5858.
25. Chu, H.-A., Debus, R. J., and Babcock, G. T. (2001) D1-Asp170 is Structurally Coupled to the Oxygen Evolving Complex in Photosystem II as Revealed by Light-Induced Fourier Transform Infrared Difference Spectroscopy, *Biochemistry 40*, 2312−2316.
26. Debus, R. J., Aznar, C., Campbell, K. A., Gregor, W., Diner, B. A., and Britt, R. D. (2003) Does Aspartate 170 of the D1 Polypeptide Ligate the Manganese Cluster in Photosystem II? An EPR and ESEEM Study, *Biochemistry 42*, 10600−10608.
27. Vrettos, J. S., and Brudvig, G. W. (2002) Water Oxidation Chemistry of Photosystem II, *Philos. Trans. R. Soc. London, Ser. B 357*, 1395−1405.
28. McEvoy, J. P., and Brudvig, G. W. (2004) Structure-Based Mechanism of Photosynthetic Water Oxidation, *Phys. Chem. Chem. Phys. 6*, 4754−4763.
29. Messinger, J. (2004) Evaluation of Different Mechanistic Proposals for Water Oxidation in Photosynthesis on the Basis of Mn_4O_xCa Structures for the Catalytic Site and Spectroscopic Data, *Phys. Chem. Chem. Phys. 6*, 4764−4771.
30. Lundberg, M., and Siegbahn, P. E. M. (2004) Theoretical Investigations of Structure and Mechanism of the Oxygen-Evolving Complex in PSII, *Phys. Chem. Chem. Phys. 6*, 4772−4780.
31. Mäntele, W. (1996) Infrared and Fourier-Transform Infrared Spectroscopy, in *Biophysical Techniques in Photosynthesis* (Amesz, J., and Hoff, A. J., Eds.) pp 137−160, Kluwer Academic Publishers, Dordrecht, The Netherlands.
32. Vogel, R., and Siebert, F. (2000) Vibrational Spectroscopy as a Tool for Probing Protein Function, *Curr. Opin. Chem. Biol. 4*, 518−523.
33. Barth, A., and Zscherp, C. (2002) What Vibrations Tell Us About Proteins, *Q. Rev. Biophys. 35*, 369−430.
34. Noguchi, T., and Sugiura, M. (2001) Flash-Induced Fourier Transform Infrared Detection of the Structural Changes during the S-State Cycle of the Oxygen-Evolving Complex in Photosystem II, *Biochemistry 40*, 1497−1502.
35. Hillier, W., and Babcock, G. T. (2001) S-State Dependent FTIR Difference Spectra for the Photosystem II Oxygen Evolving Complex, *Biochemistry 40*, 1503−1509.
36. Noguchi, T., and Sugiura, M. (2002) Flash-Induced FTIR Difference Spectra of the Water Oxidizing Complex in Moderately Hydrated Photosystem II Core Films: Effect of Hydration Extent on S-State Transitions, *Biochemistry 41*, 2322−2330.
37. Noguchi, T., and Sugiura, M. (2002) FTIR Detection of Water Reactions During the Flash-Induced S-State Cycle of the Photosynthetic Water-Oxidizing Complex, *Biochemistry 41*, 15706−15712.
38. Noguchi, T., and Sugiura, M. (2003) Analysis of Flash-Induced FTIR Difference Spectra of the S-State Cycle in the Photosynthetic Water-Oxidizing Complex by Uniform ^{15}N and ^{13}C Isotope Labeling, *Biochemistry 42*, 6035−6042.
39. Yamanari, T., Kimura, Y., Mizusawa, N., Ishii, A., and Ono, T.-A. (2004) Mid- to Low-Frequency Fouier Transform Infrared Spectra of S-State Cycle for Photosynthetic Water Oxidation in *Synechocystis* sp. PCC 6803, *Biochemistry 43*, 7479−7490.
40. Chu, H.-A., Hillier, W., and Debus, R. J. (2004) Evidence that the C-Terminus of the D1 Polypeptide is Ligated to the Manganese Ion that Undergoes Oxidation During the S_1 to S_2 Transition: An Isotope-Edited FTIR Study, *Biochemistry 43*, 3152−3166.
41. Noguchi, T., Inoue, Y., and Tang, X.-S. (1999) Structure of a Histidine Ligand in the Photosynthetic Oxygen-Evolving Complex as Studied by Light-Induced Fourier Transform Infrared Spectroscopy, *Biochemistry 38*, 10187−10195.
42. Hasegawa, K., Ono, T.-A., and Noguchi, T. (2000) Vibrational Spectra and Ab Initio DFT Calculations of 4-Methylimidazole and Its Different Protonation Forms: Infrared and Raman Markers of the Protonation State of a Histidine Side Chain, *J. Phys. Chem. B 104*, 4235−4265.
43. Chasteen, N. D., and Harrison, P. M. (1999) Mineralization in Ferritin: An Efficient Means of Iron Storage, *J. Struct. Biol. 126*, 182−194.
44. Theil, E. C. (2000) Ferritin, in *Handbook of Metalloproteins* (Messerschmidt, A., Huber, R., Poulos, T. L., and Wieghardt, K., Eds.) pp 771−781, John Wiley & Sons, Chichester, U.K.
45. Liang, W. C., Roelofs, T. A., Cinco, R. M., Rompel, A., Latimer, M. J., Yu, W. O., Sauer, K., Klein, M. P., and Yachandra, V. K. (2000) Structural Change of the Mn Cluster During the $S_2 \rightarrow S_3$ State Transition of the Oxygen-Evolving Complex of Photosystem II. Does it Reflect the Onset of Water/Substrate Oxidation? Determination by Mn X-ray Absorption Spectroscopy, *J. Am. Chem. Soc. 122*, 3399−3412.
46. Messinger, J., and Renger, G. (1990) The Reactivity of Hydrazine with Photosystem II Strongly Depends on the Redox State of the Water Oxidizing System, *FEBS Lett. 277*, 141−146.
47. Messinger, J., Wacker, U., and Renger, G. (1991) Unusual Low Reactivity of the Water Oxidase in Redox State S_3 Toward Exogenous Reductants. Analysis of the NH_2OH- and NH_2NH_2-Induced Modifications of Flash-Induced Oxygen Evolution in Isolated Spinach Thylakoids, *Biochemistry 30*, 7852−7862.
48. Robblee, J. H., Messinger, J., Cinco, R. M., McFarlane, K. L., Fernandez, C., Pizarro, S. A., Sauer, K., and Yachandra, V. K.

(2002) The Mn Cluster in the S_0 State of the Oxygen-Evolving Complex of Photosystem II Studied by EXAFS Spectroscopy: Are There Three Di-μ-oxo-bridged Mn_2 Moieties in the Tetranuclear Mn Complex?, *J. Am. Chem. Soc. 124*, 7459−7471.

49. Glatzel, P., Bergmann, U., Yano, J., Visser, H., Robblee, J. H., Gu, W., De Groot, F. M. F., Christou, G., Pecoraro, V. L., Cramer, S. P., and Yachandra, V. K. (2004) The Electronic Structure of Mn in Oxides, Coordination Complexes, and the Oxygen-Evolving Complex of Photosystem II Studied by Resonant Inelastic X-ray Scattering, *J. Am. Chem. Soc. 126*, 9946−9959.
50. Chu, H.-A., Sackett, H., and Babcock, G. T. (2000) Identification of a Mn−O−Mn Cluster Vibrational Mode of the Oxygen-Evolving Complex in Photosystem II by Low-Frequency FTIR Spectroscopy, *Biochemistry 39*, 14371−14376.

BI047558U